



Dehazing Based on Long-Range Dependence of Foggy Images

Hong Xu Yuan¹, Zhiwu Liao^{1*}, Rui Xin Wang¹, Xinceng Dong¹, Tao Liu¹, Wu Dan Long², Qing Jin Wei¹, Ya Jie Xu¹, Yong Yu³, Peng Chen^{4,5*} and Rong Hou^{4,5*}

¹School of Computer Science, Sichuan Normal University, Chengdu, China, ²School of Computing and Artificial Intelligence, Southwest Jiaotong University, Chengdu, China, ³School of Mathematics and Computer (Big Data Science), Panzhihua University, Panzhihua, China, ⁴Chengdu Research Base of Giant Panda Breeding, Sichuan Key Laboratory of Conservation Biology for Endangered Wildlife, Chengdu, China, ⁵Sichuan Academy of Giant Panda, Chengdu, China

OPEN ACCESS

Edited by:

Ming Li,
Zhejiang University, China

Reviewed by:

Nan Mu,
Michigan Technological University,
United States
Junyu He,
Zhejiang University, China

*Correspondence:

Zhiwu Liao
liaoziwu@163.com
Peng Chen
capricorncp@163.com
Rong Hou
405536517@qq.com

Specialty section:

This article was submitted to
Interdisciplinary Physics,
a section of the journal
Frontiers in Physics

Received: 04 December 2021

Accepted: 10 January 2022

Published: 16 February 2022

Citation:

Yuan HX, Liao Z, Wang RX, Dong X,
Liu T, Long WD, Wei QJ, Xu YJ, Yu Y,
Chen P and Hou R (2022) Dehazing
Based on Long-Range Dependence of
Foggy Images.
Front. Phys. 10:828804.
doi: 10.3389/fphy.2022.828804

Deep neural networks (DNNs) with long-range dependence (LRD) have attracted more and more attention recently. However, LRD of DNNs is proposed from the view on gradient disappearance in training, which lacks theory analysis. In order to prove LRD of foggy images, the Hurst parameters of over 1,000 foggy images in SOTS are computed and discussed. Then, the Residual Dense Block Group (RDBG), which has additional long skips among two Residual Dense Blocks to fit LRD of foggy images, is proposed. The Residual Dense Block Group can significantly improve the details of dehazing image in dense fog and reduce the artifacts of dehazing image.

Keywords: long-range dependence, residual dense block, residual dense block group, deep neural network, image dehazing, Hurst parameter (H)

INTRODUCTION

The single image dehazing based on deep neural networks (DNNs) refers to restoring an image from a foggy image using DNNs. Although some efforts on dehazing have been proposed recently [1–6], foggy image modeling is still an unsolved problem.

The early image model is Gaussian or Mixture Gaussian [7], but it cannot properly fit with foggy images. In fact, the foggy images seem to show long-range dependence. That is, the gray levels seemed to influence pixels in nearby regions. In our framework, each foggy image with m rows and n columns in SOTS is reshaped as is an $m \times n$ column vector by arranging the elements of the image column by column. Thus, we can fit the images by fractional Gaussian noise (fGn) [8–12] and discuss dependence of an image by its Hurst parameter. The main conclusion of the Hurst parameter of a fGn is as follows.

The auto-correlation function (ACF) of fGn is as follows:

$$C_{fGn}(\tau) = \frac{V_H}{2} \left[(|\tau| + 1)^{2H} + (|\tau| - 1)^{2H} - 2|\tau|^{2H} \right] \quad (1)$$

where

$$V_H = \Gamma(1 - 2H) \frac{\cos \pi H}{\pi H} \quad (2)$$

is the strength of fGn and $0 < H < 1$ is the Hurst parameters [8–10].

If $0.5 < H < 1$, one has the following:

$$\int_0^{\infty} C_{fGn}(\tau) d\tau = \infty \quad (3)$$

Thus, the fGn is of long-range dependency (LRD) when $0.5 < H < 1$.

When $0 < H < 0.5$, one has the following:

$$\int_0^\infty C_{fGn}(\tau) d\tau < \infty \tag{4}$$

The above fGn is of short-range dependence (SRD) [8–12].

Recently, some deep neural networks (DNN) with LRD are proposed [4–6, 13], whose motivation is mainly from avoiding gradient disappearance in training. However, the LRD of these DNNs has never been discussed and proven in theory. In this study, the Hurst parameters of test images in SOTS datasets [14] are computed and LRD of foggy images is proven. Motivated by LRD of foggy images, we proposed a new network module, the Residual Dense Block Group (RDBG) composed of two bundled Residual Dense Block Groups (DRBs) proposed in reference [13]. The RDBG has additional long skips between two DRBs to fit LRD of foggy images and can be used to form a new dehazing network. This structure can significantly improve the quality of dehazing images in heavy fog.

The remainder of this article is as follows: the second section introduces the preliminaries of fGn; the third section gives the case study; then a framework based on LRD of foggy images is presented; finally, there are the conclusions and acknowledgments.

PRELIMINARIES

Fractional Brownian Motion

The fBm of Weyl type is defined by [8].

$$B_H(t) - B_H(0) = \frac{1}{\Gamma(H + 0.5)} \left\{ \int_{-\infty}^0 [(t-u)^{H-0.5} - (-u)^{H-0.5}] dB(u) + \int_0^t (t-u)^{H-0.5} dB(u) \right\} \tag{5}$$

where $0 < H < 1$, and $B(t)$ is Gaussian.

$$\begin{aligned} \text{fBm has stationary increment: } & B_H(t + \tau) - B_H(t) \\ &= B_H(\tau) - B_H(0) \end{aligned} \tag{6}$$

$$\text{and self-affinity property: } B_H(at) = a^H B_H(t), a > 0 \tag{7}$$

Fractional Gaussian Noise

Let $x(t)$ be the gray level of the t th pixel of an image and be a fGn [8–12].

$$x(t) = B_H(t) - B_H(0) \tag{8}$$

Its ACF follows **Eqs 1, 2**.

An approximation of $C_{fGn}(\tau)$ is as follows:

$$C_{fGn}(\tau) \propto |\tau|^{2H-2} \tag{9}$$

CASE STUDY

Data Set

Synthetic data set RESIDE: Li et al. [16] created a large-scale benchmark data set RESIDE composed of composite foggy images and real foggy images.

Synthetic data set: the SOTS test data set is used as the test set. The SOTS test set includes 500 indoor foggy images and 500 outdoor foggy images.

Real data set: it includes 100 real foggy images in the SOTS data set in the RESIDE and the real foggy data collected on the Internet.

Calculate Hurst Parameter

Rescaled range analysis (RRA) [15] for foggy images is closely associated with the Hurst exponent, H , also known as the “index of dependence” or the “index of long-range dependence.” The steps to obtain the Hurst parameter are as follows:

1. Preprocessing: An image with m row and n column is concatenated column by column to form an $m \times n$ column vector. For better understanding, a simple example is presented: the size of the foggy image in **Figure 4A** is 348×248 , and then it is concatenated column by column to form an 86,304-column vector.
2. Rescale vector: The original vector can be divided equally into several ranges for further RRA, as follows. The first range at the first layer is defined as RS_{11} , representing the original $m \times n$ vector, and then it can be divided into two parts, RS_{21} and RS_{22} , at the second layer, whose dimension equals to $(m \times n / 2)$ where $(.)$ represents the floor integer. Repeat the above process until the vector dimensions at a specific layer are less than $(m \times n / 2^6)$.

Layer 1. RS_{11} : original $m \times n$ vector.

Layer 2. RS_{21} : $(m \times n / 2)$, RS_{22} : $(m \times n / 2)$.

Layer 3. RS_{31} : $(m \times n / 4)$, RS_{32} : $(m \times n / 4)$, RS_{33} : $(m \times n / 4)$, RS_{34} : $(m \times n / 4)$.

Thus, the dimensions of ranges of the foggy image are as follows:

Layer 1. RS_{11} : 86,304.

Layer 2. RS_{21} : 43,152, RS_{22} : 43,152.

Layer 3. RS_{31} : 21,576, RS_{32} : 21,576, RS_{33} : 21,576, RS_{34} : 21,576.

3. Calculate the mean for each range.

$$m_{ij} = \frac{1}{n_{ij}} \sum_{k_{ij}=1}^{n_{ij}} X_{k_{ij}} \tag{10}$$

where n_{ij} represents the number of the elements in the j th range of the i th layer; $X_{k_{ij}}$ represents the value of the k_{ij} th element in the j th range of the i th layer; m_{ij} represents the mean value of the elements in the j th range of the i th layer.

4. Calculate the deviations of each element in every range. The deviation can be calculated as follows:

TABLE 1 | Some intermediate results of calculating the Hurst parameter of the foggy image in **Figure 5A**.

Layer	Numbers of ranges in layers	Numbers of data points in ranges (x)	Log(x)	R/S	Log (R/S)	Slope of the fitted straight line (i.e., the value of Hurst parameter)
1	1	86,304	10.6725	25,754	15.3667	0.990
2	2	43,152	9.9793	16,445	14.9181	
3	4	21,576	9.2862	7,367	14.1151	
4	8	10,788	8.5930	3,567	13.3899	
5	16	5,394	7.8999	1784	12.6969	

$$Y_{k_{ij}} = X_{k_{ij}} - m_{ij} \tag{11}$$

where $Y_{k_{ij}}$ represents the deviation of the k_{ij} th element in the j th range of the i th layer.

5. Obtain the accumulated deviations for each element in the corresponding range.

$$y_{ij,N} = \sum_{k_{ij}=1}^N Y_{k_{ij}}, \quad N = 1, \dots, n_{ij} \tag{12}$$

where $y_{ij,N}$ represents the accumulated deviation for N elements in the j th range of the i th layer.

6. Calculate the widest difference of the deviations in each range.

$$R_{ij} = \max(y_{ij,1}, y_{ij,2} \dots y_{ij,N}) - \min(y_{ij,1}, y_{ij,2} \dots y_{ij,N}), \quad N = 1, \dots, n_{ij} \tag{13}$$

where R_{ij} represents the widest difference for the j th range of the i th layer.

7. Calculate the rescaled range for each range.

$$\text{Rescaled range} = \left(\frac{R}{S}\right)_{ij} = \frac{R_{ij}}{\sigma_{ij}} \tag{14}$$

where R/S represents the rescaled range for the j th range of the i th layer, while σ_{ij} represents the standard deviation of the accumulated deviations for the j th range of the i th layer.

8. Obtain the averaged rescaled range values for each layer.

$$\left(\frac{R}{S}\right)_i = \frac{1}{2^{l-1}} \sum_{j=1}^{[m \times n / 2^{l-1}]} \left(\frac{R}{S}\right)_{ij} \tag{15}$$

where l is the layer of the ranges with the identity size. The R/S is calculated using **Eq. 15** and the R/S of the example image is shown in **Table 1**.

9. Obtain the Hurst exponent. Plot the logarithm of the size (x axis) of each range in the i th layer versus the logarithm of the average rescaled range of the corresponding layer using **Eq. 15** (y axis) (**Figure 1**), and the slope of the fitted line is regarded as the value of the Hurst exponent, that is, the Hurst parameter.

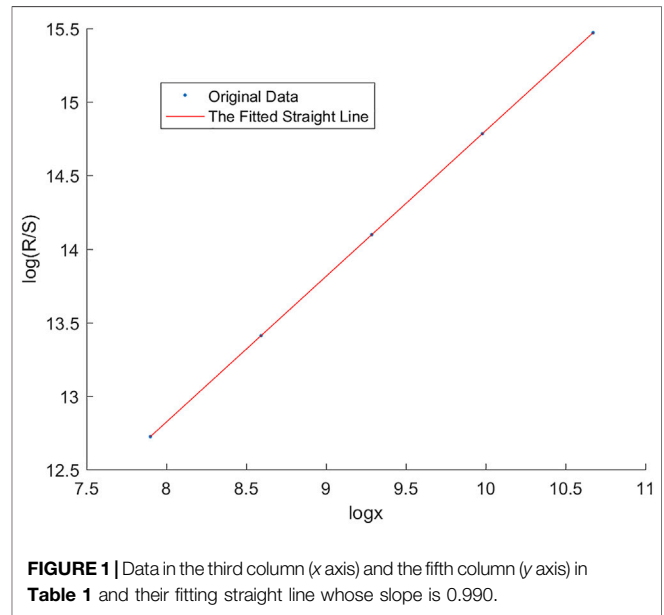


FIGURE 1 | Data in the third column (x axis) and the fifth column (y axis) in **Table 1** and their fitting straight line whose slope is 0.990.

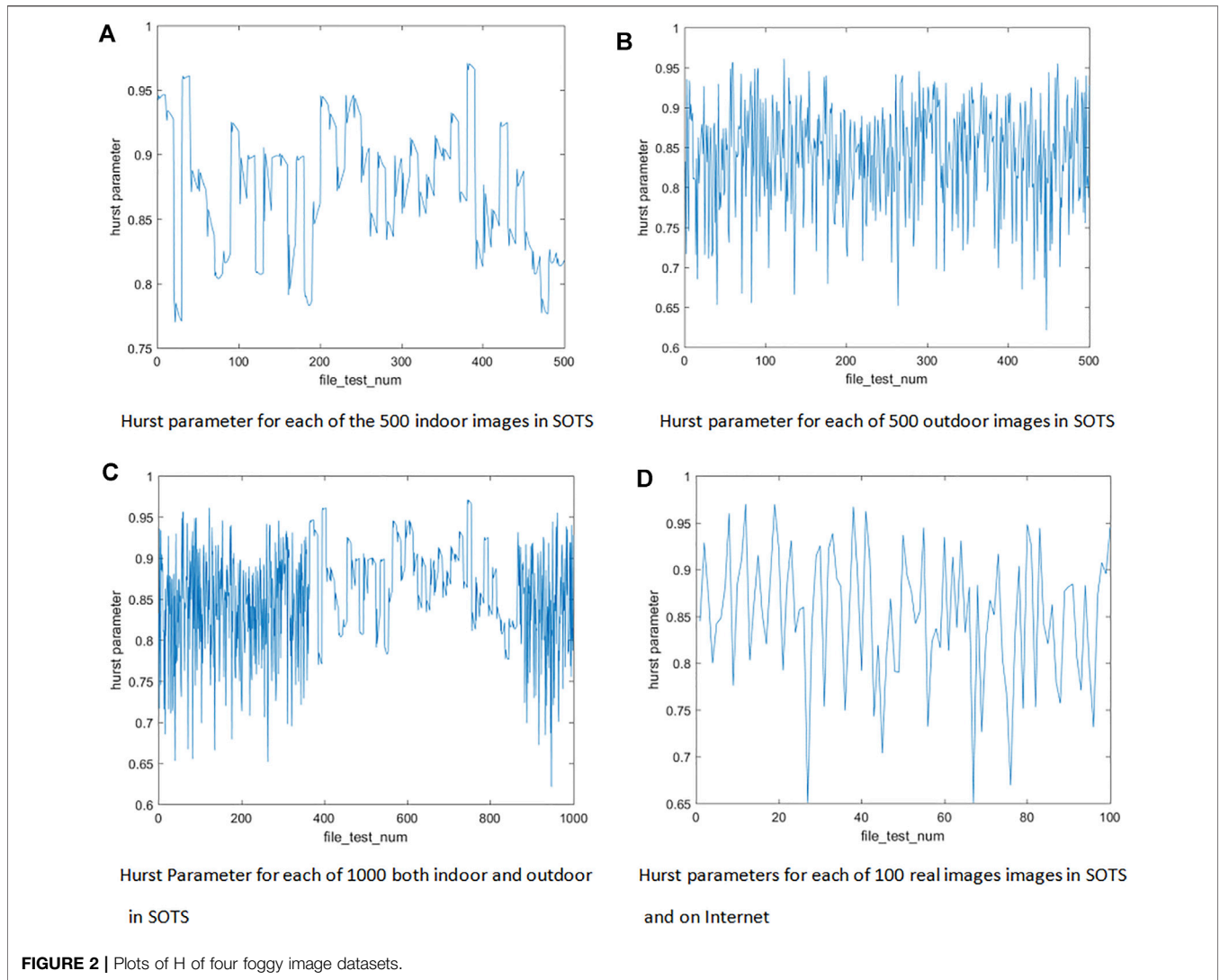
Hurst Parameters H of Foggy Images

The plots of four image sets in SOTS, 500 indoor images, 500 outdoor, 1,000 outdoor and indoor images, and 100 real foggy images, are shown in **Figure 2**. The x axis represents the serial numbers of the test images while the y axis is the Hurst parameters of the images. That is, the i th point in **Figure 2** represents the Hurst parameter of the i th image. Thus, we can know the Hurst parameters of over 1,000 foggy images by observing y values of the points in **Figure 2**.

From **Figure 2**, we can observe that the least y values of subfigures in **Figure 2** are 0.6 or 0.65, which means that the Hurst parameters of four image data sets are all above 0.6. Thus the foggy images are of LRD, which can help us design some novel dehazing methods.

Moreover, although the Hurst parameter for each image is a constant, the different images have different Hurst parameters because of their different contents. For example, the Hurst parameter of a complex image with more colors and objects (**Figures 5A,B**) is bigger than a simple image (**Figure 5C**).

Based on the LRD of the foggy images, the Residual Dense Block Group (RDBG) based on RDB is proposed. The RDBG,



which has additional long skips between two RDBs to fit LRD of foggy images, can significantly improve the details of dehazing image in dense fog and reduce the artifacts of dehazing image.

DEHAZING BASED ON RESIDUAL DENSE BLOCK GROUP

Dependence in Neural Network

The neural network can be considered as a hierarchical graph model whose nodes are connected by weighted edges. The weights of edges are trained according to some predefined cost functions. Generally, the value of the i th node in the k th layer is decided by the nodes in the $(k-1)$ th layer connected to the i th node [18–24]. That is,

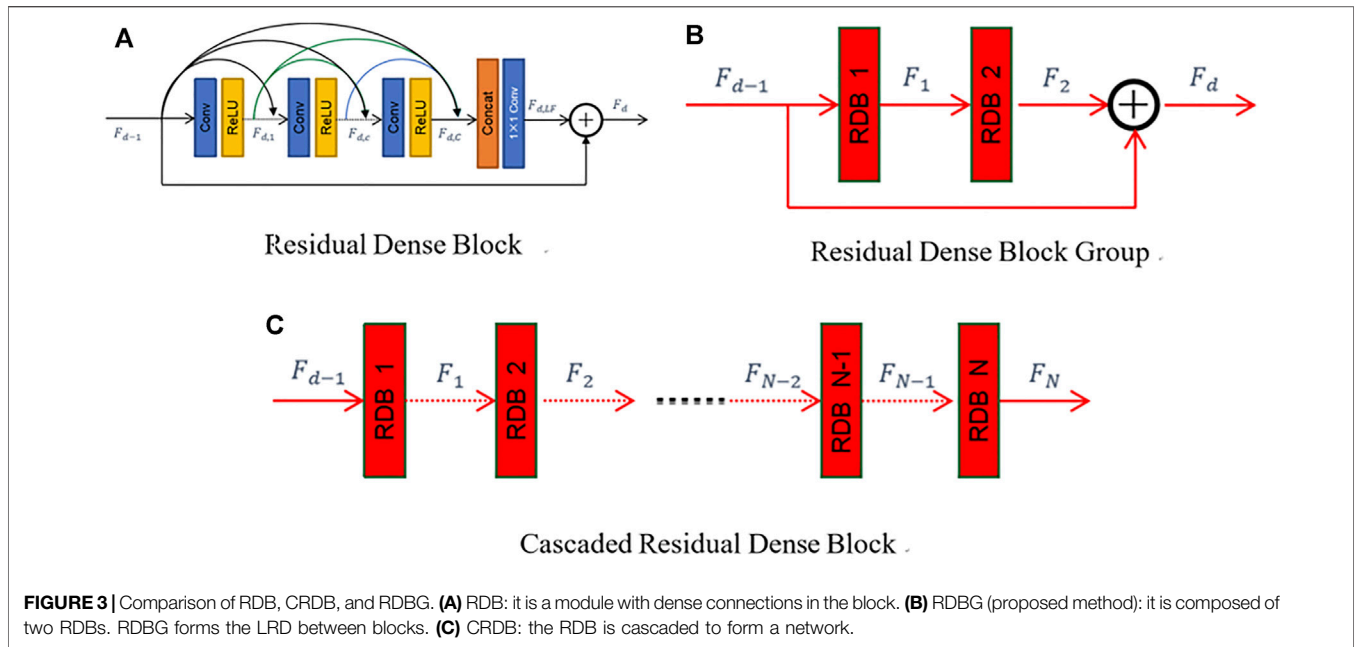
$$x^{(k)}(i) = f(W^{(k-1,k)}(i)x^{(k-1)}(i)) \quad (16)$$

where $x^{(k)}(i)$ is the value of the i th node in the k th layer, f is an activation function, $W^{(k-1,k)}$ is a vector of weights of edges to connect nodes in the $(k-1)$ th layers and the i th node, and $x^{(k-1)}(i)$ are values of nodes in the $(k-1)$ th layers connected to the i th node.

Thus, the value of the i th node is only influenced by its directly connected nodes. This assumption may be correct in some cases, but it is not true in images since we have proved the LRD of foggy images. Thus, we should design a new module of the neural network to fit the LRD of the foggy images.

Residual Dense Block Group

Just as discussed in the above subsection, the most straight method to design a structure fitting LRD of images is to connect a node to nodes with longer distance to it directly. Thus, the information of faraway nodes is introduced to help us to recover the real gray level from foggy observations.



Following this intuitive explanation, the length of a skip (connection edge between two nodes) which is defined as the number of crossing nodes can be used to measure the dependence of a time series approximately.

In this context, motivated by the LRD of foggy images, a new residual module RDBG is proposed by two bundled resident dense blocks (RDBs). As shown in **Figure 3A**, the RDB is a module with dense connections only in the block. In **Figure 3**, the features which are values of nodes in different layers of the RDB form a time series. Thus, an RDB only with dense connections in blocks cannot fit the LRD well, especially in dense fog, while the proposed RDBG which adds an additional long skip from the beginning of the first block to the end of the second block can fit the LRD better than the RDB. In heavy fog, since the RDBG fits LRD of images to utilize more information of images, it can obtain a better dehazing image.

As shown in **Figure 3C**, Yang Aiping [16] et al. and X Liu [17] et al. used consecutive RDBs in a cascade manner. Since connections are also in blocks, in essence, it cannot fit LRD of images well.

Experimental Results and Discussions

The method proposed in this article will be compared with four state-of-the-art dehazing methods: DehazeNet, AOD-Net, DCP, and GFN.

Three metrics: PSNR, SSIM, and reference-less FADE are used to evaluate the quality of dehazing images. Our proposed method gets the best PSNR and SSIM among all methods (**Table 2**), which means that our method has the largest similarities between the original images and the dehazing images in both image gray levels and image structures. It also has satisfied results in FADE (**Table 2**; **Figure 4**), which means that our method is robust and stable in dehazing.

TABLE 2 | PSNR, SSIM, and FADE between the dehazing results and original images of synthetic image in SOATS. The best results are marked by bold.

Dataset	Metric	DCP	DehazeNet	AOD-net	GFN	OURS1
Indoor	PSNR	16.16	19.82	20.15	24.91	28.479
	SSIM	0.8546	0.8209	0.8162	0.9186	0.9665
	FADE	0.7792	0.7943	0.8052	0.5364	0.5602
Outdoor	PSNR	19.14	24.75	24.14	28.29	30.033
	SSIM	0.8605	0.9269	0.9181	0.9621	0.9714
	FADE	0.5941	0.7671	0.7677	0.8238	0.7442

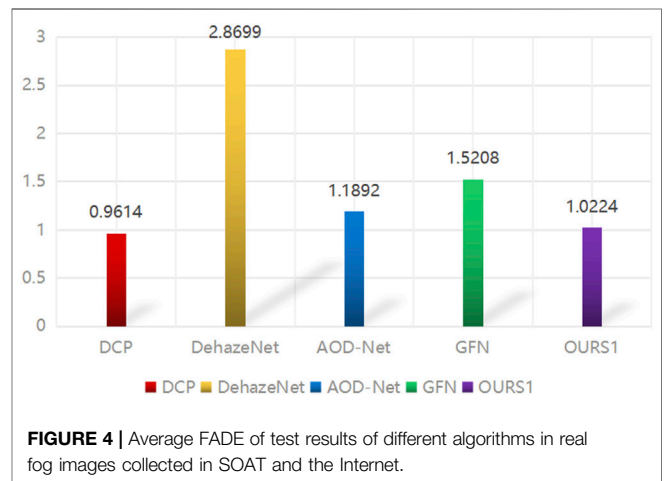


FIGURE 4 | Average FADE of test results of different algorithms in real fog images collected in SOAT and the Internet.

The dehazing examples are given in **Figures 5, 6**, and their Hurst parameters are given under the foggy images.

	A	B	C
Foggy image			
	H=0.990	H=0.933	H=0.876
Original image			
AOD			
	PSNR=20.44, SSIM=0.85, fADE=0.80	PSNR=18.36, SSIM=0.89, fADE=0.78	PSNR=25.43, SSIM=0.91, fADE=0.76
DCP			
	PSNR=18.03, SSIM=0.83, fADE=0.78	PSNR=17.07, SSIM=0.76, fADE=0.79	PSNR=20.05, SSIM=0.89, fADE=0.59
DehazNet			
	PSNR=20.84, SSIM=0.85, fADE=0.80	PSNR=19.16, SSIM=0.90, fADE=0.81	PSNR=25.33, SSIM=0.94, fADE=0.77
GFN			
	PSNR=24.51, SSIM=0.92, fADE=0.52	PSNR=26.96, SSIM=0.96, fADE=0.53	PSNR=29.73, SSIM=0.95, fADE=0.82
Proposed method			
	PSNR=30.85, SSIM=0.98, fADE=0.53	PSNR=30.36, SSIM=0.98, fADE=0.53	PSNR=30.00, SSIM=0.95, fADE=0.74

FIGURE 5 | Some dehazing images and their image quality metrics of synthetic foggy data in SOATS.




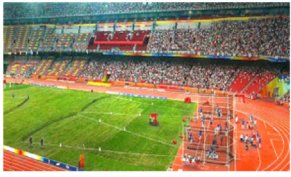


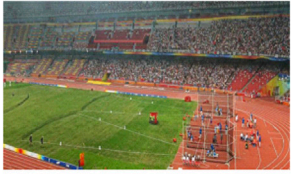


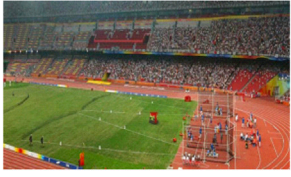


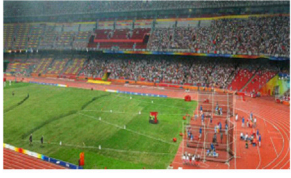

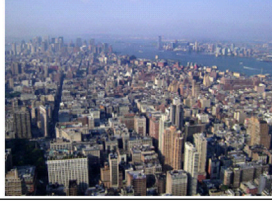
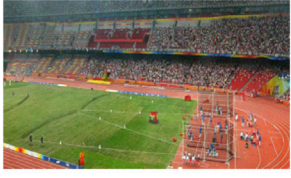


	A	B	C
Foggy image			
DCP			
	FADE=0.99	FADE=0.99	FADE=0.94
AOD			
	FADE=1.33	FADE=1.41	FADE=1.05
DehazNet			
	FADE=2.50	FADE=2.89	FADE=1.99
GFN			
	FADE=1.49	FADE=1.60	FADE=1.33
Proposed method			
	FADE=1.25	FADE=1.01	FADE=0.97

FIGURE 6 | Some dehazing images and their image quality metrics of real foggy data in SOATS and on the Internet.

CONCLUSION

Assuming the foggy images are of fGn and calculating their Hurst parameters, the LRD of over 1,000 foggy

images are proven by the fact that their Hurst parameters are all more than 0.6. Motivated by the LRD of foggy images, the Residual Dense Block Group (RDBG) with additional long skips between two RDBs is proposed. The

RDBG utilizes information of LRD foggy images well and can obtain satisfied dehazing images.

DATA AVAILABILITY STATEMENT

The original contributions presented in the study are included in the article/Supplementary Material; further inquiries can be directed to the corresponding authors.

REFERENCES

- Cai B, Xu X, Jia K, Qing C, Tao D DehazeNet: An End-To-End System for Single Image Haze Removal. *IEEE Trans Image Process* (2016) 25(11):5187–98. doi:10.1109/tip.2016.2598681
- Li B, Peng X, Wang Z, Xu J, Feng D. AOD-net: All-In-One Dehazing Network [C]. In: Proceeding of the 2017 IEEE International Conference on Computer Vision (ICCV); 22–29 Oct. 2017; Venice, Italy. IEEE (2017). p. 4780–8. doi:10.1109/iccv.2017.511
- Zhang H, Patel VM. Densely Connected Pyramid Dehazing Network[C]. In: Proceeding of the 2018 IEEE/CVF Conference on Computer Vision and Pattern Recognition (CVPR); 18–23 June 2018; Salt Lake City, UT, USA. IEEE (2018). p. 3194–203. doi:10.1109/CVPR.2018.00337
- Hochreiter S, Schmidhuber J Long Short-Term Memory. *Neural Comput* (1997) 9:1735–80. doi:10.1162/neco.1997.9.8.1735
- Zaremba W, Sutskever I, Vinyals O. RECURRENT NEURAL NETWORK REGULARIZATION. In: International Conference on Learning Representations (ICLR) 2015; 2015 May 7–9; San Diego, CA (2014).
- Ren W, Ma L, Zhang J, Pan J, Cao X, Liu W, et al. Gated Fusion Network for Single Image Dehazing [J]. *Proc IEEE Conf Computer Vis Pattern Recognition(CVPR)* (2018), p. 3253–3261. doi:10.1109/CVPR.2018.00343
- Liao Z, Tang YY. Signal Denoising Using Wavelet and Block Hidden Markov Model. *Int J Pattern Recognition Artif Intelligence* (2005) 19(No. 5):681–700. doi:10.1142/s0218001405004265
- Li M Modified Multifractional Gaussian Noise and its Application. *Physica Scripta* (2021) 96(12):125002. doi:10.1088/1402-4896/ac1cf6
- Li M Generalized Fractional Gaussian Noise and its Application to Traffic Modeling. *Physica A* (2021) 579:1236137. doi:10.1016/j.physa.2021.126138
- Li M Multi-fractional Generalized Cauchy Process and its Application to Teletraffic. *Physica A: Stat Mech its Appl* (2020) 550:123982. doi:10.1016/j.physa.2019.123982
- He J, George C, Wu J, Li M, Leng J. Spatiotemporal BME Characterization and Mapping of Sea Surface Chlorophyll in Chesapeake Bay (USA) Using Auxiliary Sea Surface Temperature Data. *Sci Total Environ* (2021) 794:148670. doi:10.1016/j.scitotenv.2021
- He J Application of Generalized Cauchy Process on Modeling the Long-Range Dependence and Self-Similarity of Sea Surface Chlorophyll Using 23 Years of Remote Sensing Data. *Front Phys* (2021) 9:750347. doi:10.3389/fphy.2021.750347
- Zhang Y, Tian Y, Kong Y, Zhong B, Fu Y. Residual Dense Network for Image Super-Resolution[J]. *IEEE* (2018).
- Li B, Ren W, Fu D, Tao D, Feng D, Zeng W, et al. Benchmarking Single Image Dehazing and Beyond[J]. *IEEE Trans Image Process* (2017) 28(1):492–505. doi:10.1109/TIP.2018.2867951

AUTHOR CONTRIBUTIONS

All authors listed have made a substantial, direct, and intellectual contribution to the work and approved it for publication.

FUNDING

The Chengdu Research Base of Giant Panda Breeding, Grant/Award Number: 2020CPB-C09, CPB2018-01, 2021CPB-B06, and 2021CPB-C01.

- Hurst HE Long-term Storage Capacity of Reservoirs. *T Am Soc Civ Eng* (1951) 116:770–99. doi:10.1061/taceat.0006518
- Yang A-P, Jin L, Jin-Jia X, Xiao-Xiao L, He Y-Q. Content Feature and Style Feature Fusion Network for Single Image Dehazing. *ACTA Automatica Sinica* (2021) 1–11. [2021-03-25]. doi:10.16383/j.aas.c200217
- Liu X, Ma Y, Shi Z, Chen J. GridDehazeNet: Attention-Based Multi-Scale Network for Image Dehazing [C]. In: Proceeding of the 2019 IEEE/CVF International Conference on Computer Vision (ICCV); Seoul, Korea; 2019 Oct 27–Nov 2. IEEE (2019), p. 7313–7322. doi:10.1109/ICCV.2019.00741
- Girshick R Fast R-CNN. In: IEEE International Conference on Computer Vision (ICCV); 2015 Dec 7–13; Santiago, Chile (2015). p. 1440–1448. doi:10.1109/ICCV.2015.169
- Johnson J, Alahi A, Fei-Fei L. Perceptual Losses for Real-Time Style Transfer and Super-Resolution[J]. *Computer Sci* (2016).
- Russakovsky O, Deng J, Su H, Krause J, Satheesh S, Ma S, et al. ImageNet Large Scale Visual Recognition Challenge. *Int J Comput Vis* (2015) 115(3):211–52. doi:10.1007/s11263-015-0816-y
- Simonyan K, Zisserman A. Very Deep Convolutional Networks for Large-Scale Image Recognition[J]. In International Conference on Learning Representations (ICLR); 2015 May 7–9; San Diego, CA (2014).
- Hu J, Shen L, Albanie S, Sun G, Wu E Squeeze-and-Excitation Networks[J]. *IEEE Trans Pattern Anal Machine Intelligence* (2017).
- Wang Z, Bovik AC, Sheikh HR, Simoncelli EP. Image Quality Assessment: from Error Visibility to Structural Similarity. *IEEE Trans Image Process* (2004) 13(4):600–12. doi:10.1109/tip.2003.819861
- Choi LK, Jaehee You J, Bovik AC Referenceless Prediction of Perceptual Fog Density and Perceptual Image Defogging. *IEEE Trans Image Process* (2015) 24(11):3888–901. doi:10.1109/tip.2015.2456502

Conflict of Interest: The authors declare that the research was conducted in the absence of any commercial or financial relationships that could be construed as a potential conflict of interest.

Publisher's Note: All claims expressed in this article are solely those of the authors and do not necessarily represent those of their affiliated organizations, or those of the publisher, the editors, and the reviewers. Any product that may be evaluated in this article, or claim that may be made by its manufacturer, is not guaranteed or endorsed by the publisher.

Copyright © 2022 Yuan, Liao, Wang, Dong, Liu, Long, Wei, Xu, Yu, Chen and Hou. This is an open-access article distributed under the terms of the Creative Commons Attribution License (CC BY). The use, distribution or reproduction in other forums is permitted, provided the original author(s) and the copyright owner(s) are credited and that the original publication in this journal is cited, in accordance with accepted academic practice. No use, distribution or reproduction is permitted which does not comply with these terms.